

Mineralogy of the Navachab skarn deposit, Namibia: an unusual Au-bearing skarn in high-grade metamorphic rocks

Markus F.-J. Nörtemann¹, Arno Mücke², Klaus Weber³, Lawrence D. Meinert¹

¹Department of Geology, Washington State University, Pullman, WA 99164-2812, USA,

²Institute of Mineralogy and Petrology, Georg-August-University, 37077 Göttingen, Germany

³Institute of Geology and Dynamics of the Lithosphere, Georg-August-University, 37077 Göttingen, Germany

The Navachab deposit is a reduced gold skarn in the neoproterozoic Damara Orogen in Namibia. Calc-silicate mineralogy differs from typical gold skarns; Navachab garnets are subcalcic with up to 90 mole% pyralspite and pyroxene contains up to 16 mole% johannsenite. The metasomatic zonation from marble towards skarn involves an increase in Si, Fe and Mn. Initially, the zonation reflects the protholith, a banded marble, as evidenced by growth of garnet in pelitic layers and clinopyroxene in carbonate layers. Ore mineralisation is divided into two paragenesis: stage I containing pyrrhotite, chalcopyrite, arsenopyrite and sphalerite and stage II with pyrite, maldonite, bismuth and gold. The P-T conditions were determined by sphalerite and arsenopyrite geobarometry/-thermometry. Sphalerite yields pressures of 2-2.5 kb and a temperature of 590 °C, arsenopyrite yields temperatures of 575± 15°C, correlating with the HT-LP-metamorphism in the central Damara Orogen. However, P-T-conditions of Navachab are higher compared to gold skarns directly associated with intrusions. This is consistent with deposits like Lucky Draw and Tillicum, that are hybrids between a regional metamorphic environment and Phanerozoic plutonism. A barren, camptonitic metalmagrophyre is considered to represent a redox-trap for Au-bearing fluids and its unusual, Mn- and Fe-rich composition is reflected in the skarn mineralogy.

Geological Setting

The Navachab Au deposit occurs in the southern Central Zone (sCZ) of the Damara Orogen which forms part of the Pan-African system of mobile belts (Fig. 1). The Damara-Orogen developed during the closure of the proto-South Atlantic (Porada, 1989) and consists of 3 mobile belts: the NS-trending Kaoko and Gariep Belts and the NE-trending Damara Belt. The Damara Belt is subdivided into several major tectonostratigraphic zones bounded by prominent NE-trending, multiply re-activated lineaments (Miller, 1983).

The oldest rocks in the Central Zone (CZ) of the Damara Belt (CZ, Fig. 2) are basement rocks of Eburian age that in the Abbabis Inlier contain 1925 ± 330 Ma granitoids (Jacob *et al.*, 1978). A lower age limit for the basement rocks of the Abbabis Inlier is set by a cross-cutting 900-1000 Ma metadolerite dyke swarm (Steven, 1994). The 750-550 Ma Damara metasedimentary sequence overlies the basement rocks and displays rapid facies changes, particularly in the southern part of

the Central Zone. The Damara sequence is cut by dolerite dykes associated with Etendeka volcanism and the emplacement of the Damaraland Igneous Complexes (e.g., Fig. 2, Erongo Complex; 132 Ma, Milner *et al.*, 1995).

Kröner (1982) subdivided the regional metamor-

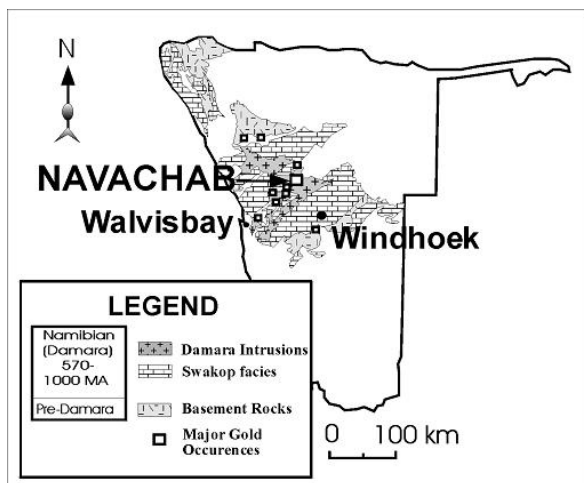


Figure 1: Geological overview of the Damara Orogen and major gold occurrences

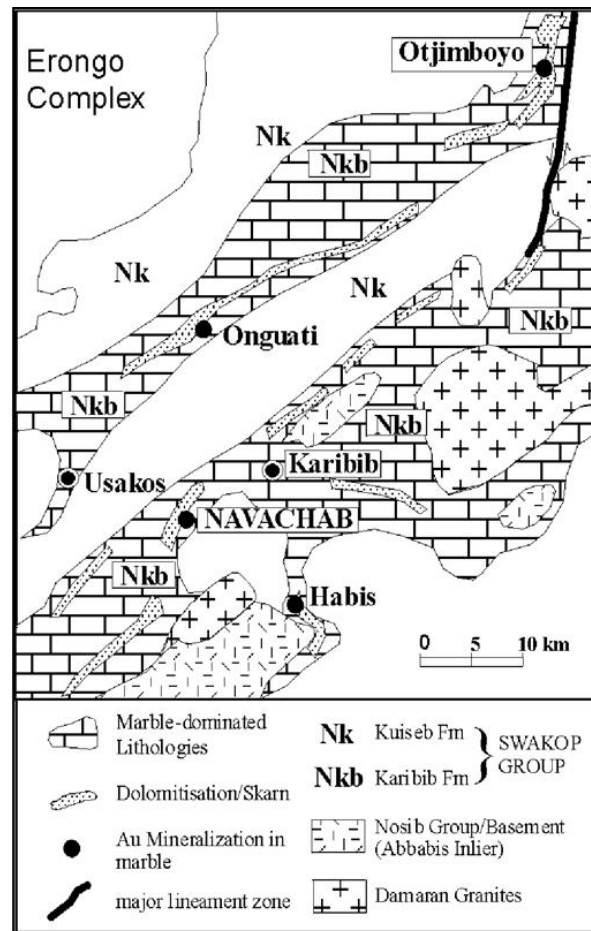


Figure 2: Gold skarn occurrences and their geological setting in the Central Zone of Damara Orogen (CZ), modified after Pirajno and Jacob (1991)

phism of the Damara-Belt into three peaks connected to periods of granitic intrusion. However Puhan (1983) and Hoffer (1983) described one long-lasting, prograde metamorphic event up to amphibolite facies, accompanied by partial melting in the southwestern part of the Damara Belt. The P-T conditions range from 2.6 kb/555°C in the NE to 3.4 kb/645°C in the SW at the Atlantic coast near Swakopmund (Puhan, 1983). Based on a petrogenetic grid on metapelites of the CZ, Steven (1994) determined pressures of 2.2–3.6 kb and temperatures of 500°C–660°C near granitic intrusions. Peak regional metamorphism occurred about 530–520 Ma (Haack *et al.* 1980; Horstmann, 1987).

The Navachab Deposit

There are several different types of ore deposits in the CZ including intrusion-hosted U- and Sn-deposits, pegmatitic REE occurrences and a variety of base and precious metal ores hosted by Damaran metasediments, many with skarn alteration (Fig. 2), such as Navachab, (Pirajno and Jacob 1991; Nörtemann, 1997), Otjimboyo (Nörtemann, 1997) and Habis (Steven, 1994).

The Navachab open-pit mine is located 10 km southwest of Karibib in the southern Central Zone (sCZ) of the Damara Belt (Figs. 2 and 3). The deposit was discovered in 1984 and production (2.3 t/y at 2.2–2.4 g/t Au, ore reserves approximately 10 Mt) started in 1989. The main ore body is hosted by the Okawayo Formation marbles, which are subdivided into three major marble horizons (Fig. 3; DM, M and MC units) and one intercalated metalamprophyre member (MCH unit, “marker hornfels”), with camptonitic geochemistry (Nörtemann, 1997). The Okawayo Formation is overlain by the biotite schists of the Oberwasser Formation and by the CM unit of the Karibib Formation. The immediate footwall is built up by siliciclastic rocks of the Spes Bona Formation, diamictite of the Chuos Formation and meta-arkose of the Etusis Formation. The units strike NE and dip 70° NW.

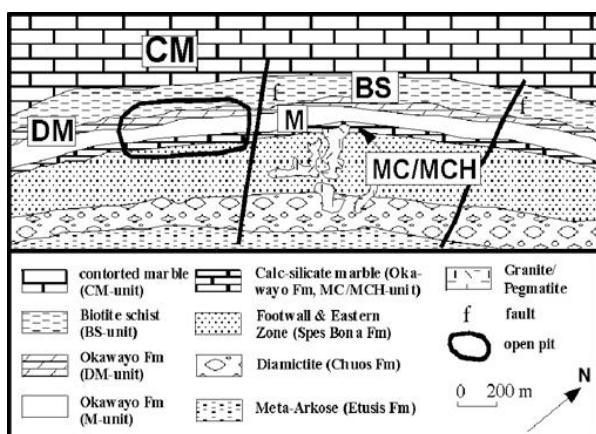


Figure 3: Geological map of the Navachab gold skarn deposit (modified after Erongo Mining, 1989).

Gold mineralisation is stratabound within the marbles but occurs both disseminated in skarn and as discordant, en echelon veins. Most economic mineralisation is hosted by the MC unit (calc-silicate rich, Fig. 3) at the base of the Okawayo Formation, immediately underlying the metalamprophyre. Gold occurs mainly as native gold, with minor maldonite (Au_2Bi) and solid solution in bismuth (up to 4 mole % Au, Nörtemann, 1997). The metalamprophyre MCH member is in general barren of gold.

Alteration

The skarn is mineralogically zoned and reflects the composition of the protolith, including the Okawayo marbles (M and MC units), followed by zones of initial skarn formation (“transition zones”) and finally zones of massive skarn alteration (MC unit). The zonation from a nearly unaltered metamorphic marble to massive skarn can be observed at both outcrop and microscopic scale because the skarn forms bands in the MC unit barely exceeding 1 m of thickness. Due to its importance for mineralisation, the metalamprophyre (MCH unit) will be described separately.

Banded marble (M and MC units)

In the initial stage of skarn development, the mineralogy reflects the composition of the protolith, which is a banded, calcitic marble with dark biotite-enriched layers and white calcitic layers.

Evidence for this is the preferred growth of early aluminous garnet in biotite- and feldspar-enriched pelitic layers and of aluminum-poor clinopyroxene in mainly carbonate layers (Fig. 4). The original marble banding is well preserved during ongoing metasomatism. The carbonate-rich layers exhibit a re-equilibration texture and contain minor feldspar, biotite, tremolite and chlorite. Compositionally, the carbonate consists of ≥ 92 mole% calcite, 3–4 mole% magnesite, and 1–2 mole% rhodochrosite and siderite. Amphibole is of tremolitic

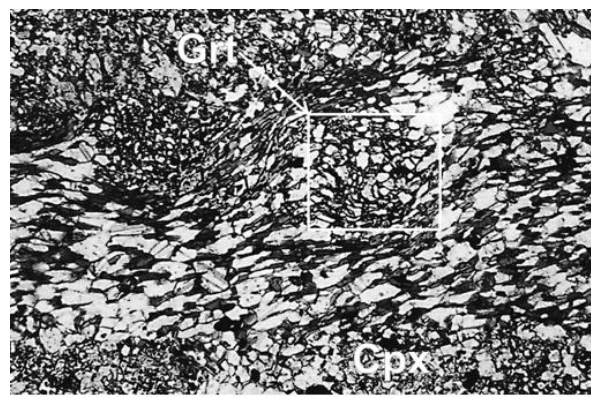


Figure 4: Early poikiloblastic garnet (Grt) preferably growing in biotitic layers shows locally helicitic structures (rectangle). Clinopyroxene (Cpx) replaces carbonate in the white calcite layers. Lower edge=1.4 mm.

composition. The dark biotite layers are fine grained and foliated. Biotite is accompanied by carbonate, amphibole, quartz and locally garnet. Early, subhedral garnet replaces the phlogopitic biotite and contains roughly equal parts grossularite, spessartite and almandine (Table 1), in reasonable isochemical balance with the replaced feldspar, biotite and carbonate protolith.

Transition zones

Initial metasomatism is indicated by the first occurrence of clinopyroxene replacing carbonate and by the growth of a second, massive garnet (Grt and Cpx in Fig. 4, Grt I in Fig. 5). These rocks display signatures of both metamorphic marble and metasomatic skarn and thus are described as transition zones. Furthermore, helicitic structures in some grains are related to synkinematic growth (rectangle in Fig. 4). The massive garnet has a slightly lower grossularite content and higher spessartite, up to 38 mole % (Table 2). Generally, the subcalcic components increase during initial metasomatism. Clinopyroxene consists mainly of diopside (up to 66

mole%) with up to 6 mole% johannsenite (Table 1).

Skarn (MC unit)

Massive skarn is characterised by the development of nearly monomineralic garnet and pyroxene layers with crystals measuring up to several mm in diameter. The contact between the layers is generally sharp, although reaction borders are common (Fig. 5). Clinopyroxene consists of hedenbergite and diopside (>40 mole% each) and up to 16 mole% johannsenite (Table 1). The presence of spherulitic graphite indicates low $f(\text{O}_2)$ conditions during skarn formation (Fig. 6). Retrograde alteration of pyroxene produced Fe-actinolite, quartz and carbonate. Some grains of Mn-rich actinolite have tiroiditic compositions. The composition of carbonate in skarn displays a loss of magnesite and an increase in rhodochrosite (up to 5 mole%) relative to the original protolith. Locally, late hydrothermal veins with quartz, calcite and mineralization crosscut the skarn.

Most skarn garnet, even where not optically zoned

Table 1: Representative analyses of clinopyroxene in altered marble (transition) and weak and strongly altered clinopyroxene skarn (w.a.skarn/s.a.skarn). Upper part: weight percent, lower part: calculated end members in mole percent.

Sample Nr.	2208-3c	2208-3c	2221-11	2221-11	2204-2	2204-2
Lithology	transition	transition	w.a.skarn	w.a.skarn	s.a. skarn	s.a. skarn
SiO ₂	50.75	51.27	51.39	50.52	49.40	50.30
TiO ₂	0.62	1.08	0.00	0.00	0.00	0.00
Al ₂ O ₃	0.19	0.28	0.11	0.14	0.48	0.11
FeO	10.87	11.48	14.43	13.54	19.91	18.77
MnO	1.83	1.88	4.47	4.89	3.10	3.80
MgO	11.35	10.67	6.84	7.07	5.63	5.78
CaO	23.93	23.47	22.26	23.99	21.07	20.45
Na ₂ O	0.00	0.00	0.70	0.00	0.00	0.00
Total	99.54	100.14	100.25	100.15	99.64	99.25
Fe ₂ O ₃ (calc)	2.64	0.21	1.61	1.59	1.11	0.00
FeO (calc)	8.49	11.29	12.98	12.11	18.91	18.77
Total	99.80	100.16	100.41	100.31	99.75	99.25
Johannsenite	6.07	5.92	15.24	16.68	9.78	11.65
Hedenbergite	27.77	35.06	43.70	40.82	58.95	57.01
Diopside	66.16	59.03	41.06	42.50	31.27	31.30
Total	100.00	100.00	100.00	100.00	100.00	100.00

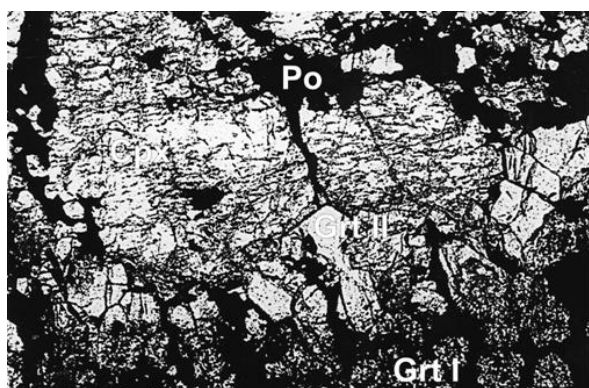


Figure 5: Strongly altered contact zone of clinopyroxene and garnet skarn. A second generation of massive garnet (Grt II) replaces pyroxene (Cpx) under supply of sulfur. Late-stage hydrothermal fractures are mineralised with pyrrhotite (Po). Lower edge=1.4 mm.

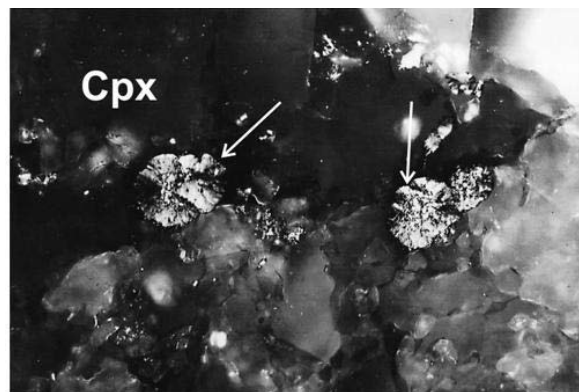
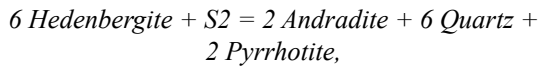


Figure 6: Spherulitic graphite precipitates (arrows) on grain boundaries of clinopyroxene (cpx) indicating reduced environment. Lower edge=1.4 mm.

Table 2: Representative analysis of garnets in marble, altered marble (transition zone) and skarn. Upper part: weight percent, lower part: calculated end members in mole percent.

Sample-Nr.	8	3	1	1	1	1
Lithology:	marble	transition	skarn	skarn	skarn	skarn
meas. area			margin	core	margin	core
SiO ₂	38.46	37.09	36.97	36.59	36.28	37.09
Ti O ₂	0.00	0.00	0.00	0.00	0.00	0.00
Al ₂ O ₃	21.78	21.06	18.23	19.27	17.29	18.86
FeO	13.88	15.10	14.57	18.39	13.97	16.69
MnO	12.75	17.11	23.67	22.42	25.19	23.95
MgO	0.82	0.70	0.52	0.63	0.25	0.15
CaO	13.25	8.47	5.13	2.15	6.48	3.73
Na ₂ O	0.00	0.00	1.26	0.00	0.00	0.00
Total	100.93	99.53	100.38	99.46	99.48	100.53
Fe ₂ O ₃ (calc)	0.00	0.00	4.48	2.02	5.15	2.97
FeO (calc)	13.88	15.14	10.54	16.57	9.33	14.02
Total	100.93	99.56	100.83	99.66	100.00	100.82
Andradite	0.00	0.00	14.40	6.32	15.95	9.24
Pyrope	3.22	2.80	2.21	2.58	1.01	0.63
Almandine	30.69	33.96	25.08	38.39	21.41	32.35
Grossularite	37.53	24.34	1.25	0.07	3.11	1.79
Spessartite	28.56	38.89	57.07	52.63	58.52	55.99
Total	100.00	100.00	100.00	100.00	100.00	100.00

is compositionally zoned with more andraditic rims. Garnet rims can contain up to 50 mole% spessartite and grossularite vanishes completely (Table 2). Garnet in the massive skarn shows a strong optical zonation, with a poikiloblastic, almandine-rich core and spessartite- and andradite-rich rims (Table 2). In general, in the garnet skarn spessartite and andradite reach the highest values. The contact of massive garnet with pyroxene skarn hosts a younger generation of garnet (Gt II in Fig. 5). Together with pyrrhotite, this garnet replaces the pyroxene. In contrast to older garnets, a chemical and microscopical zonation is not apparent. Gamble (1982) described garnet replacing pyroxene under high sulfur conditions after the reaction



that is applicable to the contact areas of garnet and pyroxene skarn.

The overall compositional trend from metamorphic to metasomatic calc-silicate minerals is a significant increase in Mn and Fe. This same trend is seen in time and space in multiple generations of skarn minerals, e.g. pyroxene and garnet (Figs. 7 and 8). There also is a trend towards more reducing conditions from marble to skarn with time, as indicated by the precipitation of graphite due to the replacement of carbonate, the decrease of the Mg-Fe ratio in amphiboles and the increase of subcalcic components in garnet (Fig. 7, Table 2). Further evidence is the complete lack of magnetite, hematite and dolomite in skarn and marble of the M and MC units.

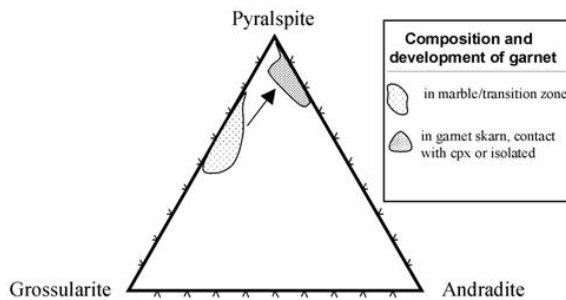


Figure 7: Increase of Mn and Fe contents in garnet from marble to massive skarn

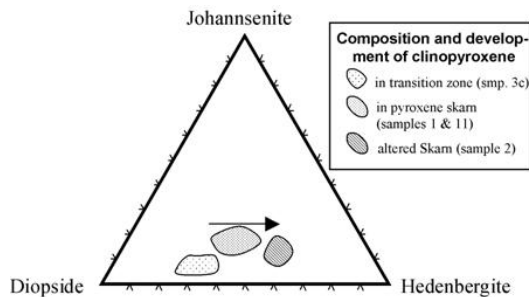


Figure 8: Increase of Mn and Fe contents in pyroxene from marble to massive skarn

Mineralisation

The ore mineralisation occurs in two different epigenetic styles: as stratiform, lense-shaped skarn bodies elongated in ENE direction and plunging about 30° to the north and as late-stage hydrothermal fractures cross-cutting the skarn (Erongo Mining, 1989). In the skarn, mineralisation is strongly associated with retrograde alteration (dominantly amphibole) and is mineralized along grain boundaries, fractures and massive replacements of garnet and pyroxene (Po in Fig. 5). Two main paragenetic sequences are distinguished in skarn ore: an older one with pyrrhotite, chalcopyrite, arsenopyrite, sphalerite and minor molybdenite, scheelite and uraninite (Fig. 9) and a younger one bearing native bismuth, gold, pyrite, bismuthinite, accompanied by remobilised pyrrhotite and chalcopyrite (Fig. 10). Due to their euhedral shape and isolated occurrence, arsenopyrite and molybdenite are assumed to represent the earliest stage of ore mineralisation.

The first paragenetic sequence is developed in the form of massive ores in fractures and veins which are interpreted to be part of the brittle regional D4-deformation stage. The massive ore is dominated by pyrrhotite (>90 vol%) which occurs together with chalcopyrite and displays locally a recrystallization texture (Fig. 9).

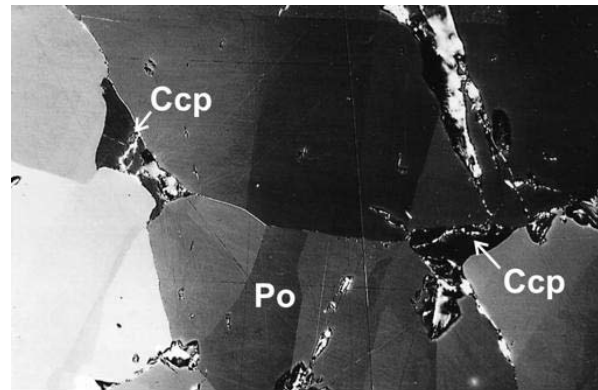


Figure 9: Pyrrhotite (Po) with equilibrated foam texture progressively replacing chalcopyrite (Ccp). Pyroxene skarn. Lower edge 0.56mm, crossed nicols.

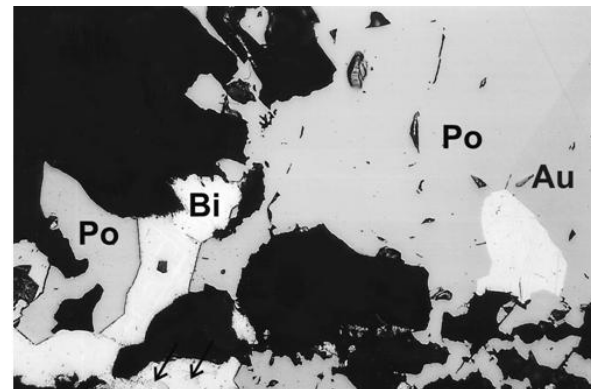


Figure 10: Native gold (Au) and bismuth (Bi) marginal to pyrrhotite (Po). Interstitial to bismuth, small alterations of bismuthinite (arrow) are visible. Lower edge=0.56 mm

Pyrrhotite reaches grain sizes up to 4 mm and commonly shows patterns of deformation, e.g. subgrains and kinking. Chalcopyrite shows no inversion twinning which indicates growth under the inversion temperature of approximately 500°C. Furthermore, chalcopyrite is associated with euhedral, early amphibole. Minor minerals include dark red to brown, relatively Fe-rich sphalerite and euhedral-subhedral arsenopyrite.

The clinopyroxene skarn hosts the main part of the younger ore paragenesis. Although volumetrically minor (< 2 vol%), it represents most of the economic mineralisation. The ore occurs in fractures and veins, and also along the margins of massive ore (Fig.10). A common feature of the younger ore is alteration of pyrrhotite and bismuth to pyrite and bismuthinite, respectively. Bismuth is spatially associated with arsenopyrite and displays a polysynthetic twinning. Bismuth commonly exhibits a recrystallization texture and locally bismuthinite infills the triple junctions. Gold reaches a grain size up to 100 µm but on average the size ranges around 10 µm.

Vein ore is volumetrically minor, but due to erratic high gold values, it is of great economic importance. It exhibits the same two paragenetic sequences as skarn ore. Differences are the increased abundance of pyrite, the lack of uraninite, molybdenite and scheelite and the presence of rutile, indicating a more oxidising environment.

Stability and genesis of ore mineralisation

The geochemical conditions of ore mineralisation at Navachab can be constrained by the composition of pyrrhotite combined with geobarometry and thermometry of sphalerite and arsenopyrite. Furthermore, the Fe content and crystal structure of pyrrhotite are related to temperature. Low Fe contents are caused by an increase of vacancies in the crystal lattice and are typical of low-temperature, monoclinic pyrrhotites. The temperature limits for intermediate and hexagonal pyrrhotite lie at 262°C and 308°C, respectively (Nakazawa and Morimoto, 1971). The pyrrhotite of Navachab displays very low Fe contents typical of monoclinic symmetry (Nörtemann, 1997). However, the fact that pyrrhotite exists in paragenesis with higher temperature chalcopyrite and sphalerite, a conversion from hexagonal to monoclinic symmetry is assumed.

According to Hutchinson and Scott (1981), the FeS content of sphalerite is related to pressure by the equation $P = 42.3 - 32.1 \cdot \log \text{FeS} [\text{mole}\%]$, with a standard deviation of ± 0.30 kbar (Fig. 11). Assuming that pyrite and pyrrhotite are co-genetic and using the most Fe-rich points as proposed by Hutchinson and Scott 1981 (up to 18 mole% Fe, Nörtemann, 1997), a pressure between 2.0 and 2.6 kb is estimated for the skarn mineralization.

The composition of arsenopyrite was measured for both skarn and quartz-dominated veins and the results

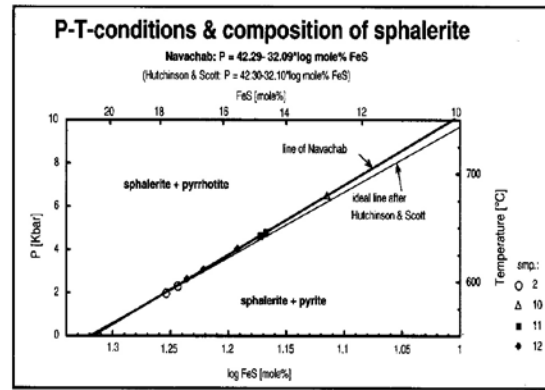


Figure 11: Results of geobarometry on sphalerite

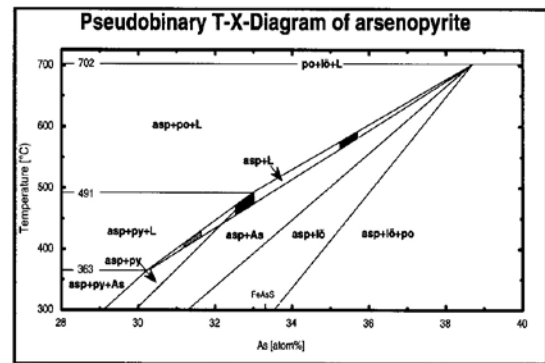


Figure 12: Results of geothermometry on arsenopyrite (dark grey area: skarn; light grey areas: quartz veins).

are plotted on the experimentally derived graph of Kretschmar and Scott (1976, Fig.12). The shaded areas in Fig. 12 indicate relatively high precipitation temperatures for the skarn (between 560-595°C) and lower temperatures in the veins (between 400-500°C), consistent with temperatures determined from sphalerite in the skarn.

Furthermore, gold in skarn displays a higher Au/Ag-ratio than in veins which is consistent with the higher solubility of Ag versus Au with decreasing temperatures. Most bismuth in skarn and veins is >99 mole% Bi but some of the skarn samples contain up to 4 mole% Au in solid solution (Nörtemann, 1997).

Mineralogy and geochemistry of the metamorphose (MCH unit)

The metamorphose is dark coloured, fine-grained and locally spotted. Towards the top, it is brecciated and bears clasts of the marble. In general, the MCH unit is barren of any economic mineralisation. Due to an intense metamorphic overprint and its geochemistry and mineralogy, this unit is termed "metamorphose".

Petrology

The dominant minerals in the metamorphose are

biotite, plagioclase, calcite, hornblende, sphene and ore minerals (pyrrhotite, chalcopyrite, sphalerite and ilmenite). The palimpsest (Spry, 1973) meta-porphyr- itic texture shows pseudomorphs after clinopyroxene, amphibole and plagioclase filled with fine-grained and untwinned plagioclase, calcite and hornblende (Figs. 13 and 14). Furthermore, they are surrounded by bands of sphene and ilmenite, where sphene replaces ilmenite. Locally, coarse-grained, twinned plagioclase represent- ing a magmatic relic is visible (Fig. 14). The premeta- morphic minerals likely contained a significant Ti- component which formed sphene and ilmenite during metamorphism.

Whole-rock geochemistry and mineral chemistry

An igneous origin of the MCH unit is interpreted from its sill-like form, undersaturation in SiO₂ expressed by the lack of quartz, and the marble breccia of the hanging wall suggesting a main kinematic event. The geochem- istry (Table 3) shows significant correlations with the data set of Rock (1991). Values of SiO₂, MgO and Na₂O are relatively low, whereas Al₂O₃, K₂O and TiO₂ are remarkably enriched. The trace elements show similar correlations, where Nb, Zr and Y are enriched and Ni

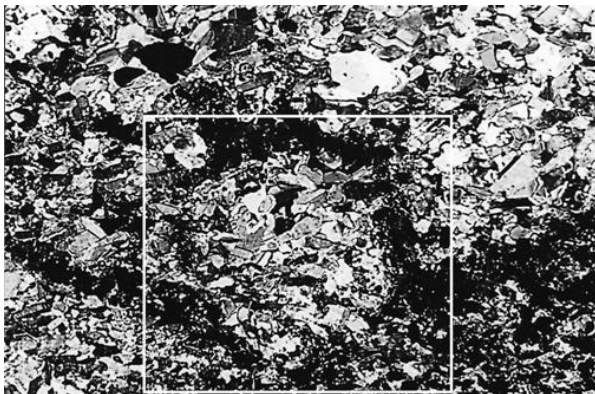


Figure 13: Palimpsest rectangle filled up with plagioclase, carbon- ate and minor biotite. The shape coincides with the basal section of amphibole. Lower edge= 1.4 mm.

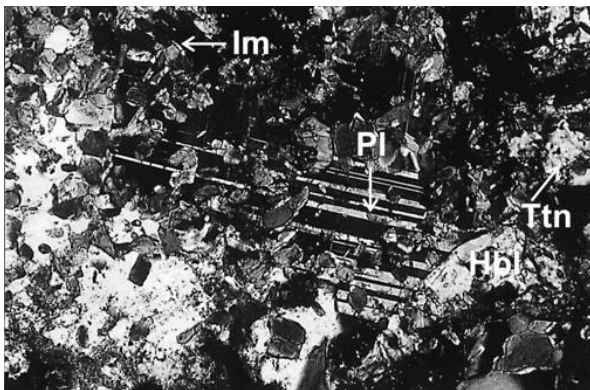


Figure 14: Palimpsest with remnants of magmatic plagioclase (Pl) replaced by biotite and hornblende (Hbl). Rims are build up by sphene (Ttn) and ilmenite (Im). Lower edge = 1.4 mm.

Table 3 : WR-geochemistry of the Navachab metalamprophyre in comparison with the data for alkaline (AL) monchiquitic (MON) and camptonitic (CAM) lamprophyres collected by Rock (1991). Analytical data given in weight percent (upper part) and ppm (lower part); n.a.: not analyzed, n.d.: not determined.

Sample	Navachab Nörtemann (1997)		AL	MON	CAM
	6b	10	average	average	average
SiO ₂	41.40	35.80	42.50	41.20	43.30
Al ₂ O ₃	15.90	16.60	13.70	13.30	14.20
Fe ₂ O ₃	1.07	1.67	n.d.	n.d.	n.d.
FeO	11.50	9.28	12.00	12.00	11.70
CaO	8.89	11.70	10.30	11.00	9.90
MgO	4.82	5.21	7.10	8.20	6.40
Na ₂ O	2.70	2.05	3.00	3.00	3.00
K ₂ O	3.94	4.26	2.00	2.00	2.10
TiO ₂	4.00	5.03	2.90	2.70	2.90
P ₂ O ₅	1.16	1.29	0.74	0.84	0.70
MnO	0.31	0.39	0.20	0.20	0.19
H ₂ O ⁻	0.16	0.17	3.1 (tot.)	3.3(tot.)	3.1(tot.)
LOI	~4	5.60	2.20	1.56	2.20
Total	99.90	99.10	99.70	99.30	99.70
Nb	130	147	101	93	97
Zr	498	553	313	270	300
Y	44	41	31	29	31
Sr	1025	802	990	1100	1050
Rb	130	142	50	46	56
Pb	15	16	22	7	9
Ga	26	28	19	15	22
Zn	79	94	98	82	90
Ni	<5	<5	65	170	50
Co	28	14	38	35	37
Cr	<5	<5	97	240	80
V	201	277	285	280	320
Ba	769	963	930	1025	850
Sc	17	24	21	21	20
Au	0.001	0.001	n.a.	n.a.	n.a.
Bi	<1	<1	n.a.	n.a.	n.a.

and Cr are extremely depleted. Furthermore, the K₂O/ Al₂O₃-Fe₂O₃/SiO₂ and V/Cr-Nb/Pb relations shown in Fig. 15 and 16 confirm the similarities to alkaline lamprophyres. The enrichment of K and Al is caused by a metasomatic overprint including the replacement of biotite and feldspar. The depletion of Si seems to suggest a metasomatic exchange of components during progressive skarn formation as well as silification of the host rock.

Diagnostic mineral assemblages

According to the geochemistry, the metalamprophyre

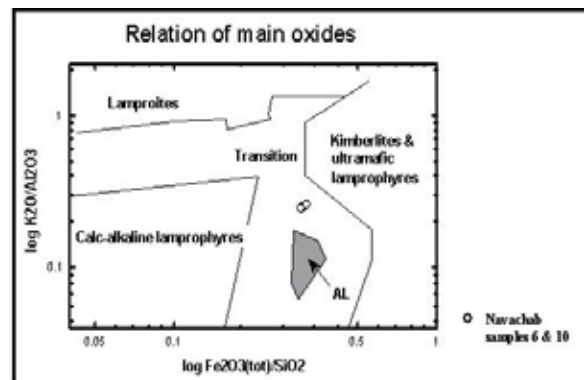


Figure 15: Discrimination of main oxides

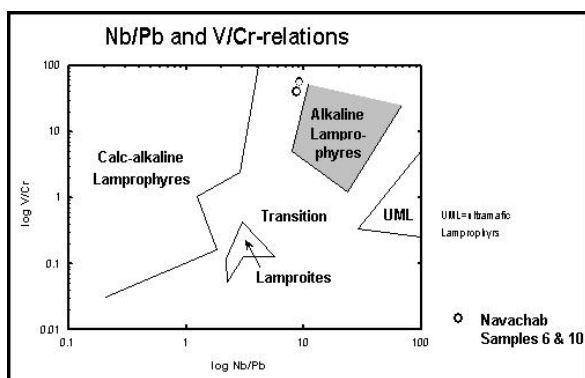


Figure 16: Nb/Pb and V/Cr relations

of Navachab is alkaline. The lack of potassium feldspar leads to the classification as camptonite. The modal mineral assemblage of magmatic camptonites consists of amphibole, biotite, plagioclase, clinopyroxene, olivine, nepheline, analcime, minor feldspar and glass. The only magmatic remnant discovered was twinned plagioclase. Most biotite in the metalamprophyre may also be magmatic. Texturally, amphibole, carbonate and sphene are of metamorphic origin, and ilmenite, Ti-rich clinopyroxene, amphibole, feldspar and analcime were replaced during metamorphism and metasomatism. The replacement origin of these minerals provides also an explanation for the lack of Ni and Cr, which would be enriched in magmatic hornblende and clinopyroxene.

Discussion and Conclusions

Navachab has many features of a typical pluton-associated gold skarn deposit but occurs in a relatively high T-P regional metamorphic environment without closely associated intrusions. Skarn at Navachab is envisioned to have formed in three stages: The first stage involves isochemical metamorphism with an exchange of volatiles, perhaps associated with the intrusion of a synmetamorphic lamprophyre sill. This caused a dehydration of the banded marble and thus an increase in fluid pressure. The second stage is characterised by further dehydration and decarbonatization with initial metasomatic transport and exchange of elements, mainly Fe and Mn, in garnet and pyroxene skarn. The development of the marble breccia is thought to be caused by the high volatile contents, possibly augmented by release of additional volatiles from the lamprophyre. The occurrence of graphite in the skarn as a product of decarbonatization implies very low oxygen fugacities, confirmed by the lack of magnetite and hematite. The third stage includes retrograde alteration, hydrothermal fracturing and precipitation of the ore. Mineralisation is a function of decreasing temperatures and increasing sulfur fugacities.

There are several other skarns in the world with similar mineralogic, metamorphic and structural features to Navachab, a group that Meinert (1998) classified as

“mesothermal“ regional metamorphic gold skarns. Examples include: Lucky Draw, Australia; Lupin, Canada; Mallapakonda and Oriental, India; Nevorita, Australia; and Tillicum, Canada..

The skarn at Tillicum (Ettlinger and Ray 1989) in Canada is developed both in metasedimentary rocks and along contacts with metabasalt; lamprophyres also occur in the vicinity of the deposit. The goldskarn mineralisation is associated with swarms of feldspar porphyry sills. The sedimentary succession comprises siliciclastics and impure marble layers and underwent sillimanite-grade metamorphism. Like Navachab, biotite predates the development of garnet and pyroxene which is replaced by late amphibole. Garnets are also of subcalcic composition with up to 55 mole% pyral-spite, pyroxenes contain up to 50 mole% hedenbergite and 8 mole% johannsenite. Furthermore, the whole-rock geochemistry shows that gold is associated with Mn oxides.

Garnet at Lucky Draw in New South Wales (Australia, Sheppard *et al.*, 1995) is mainly composed of almandine (up to 87 mole%) and pyrope (up to 37 mole%); spessartite, andradite and grossularite are absent. The skarn is hosted by quartzite and quartz-mica schist. Associated igneous rocks are shoshonitic volcanics and a fractionated I-type granite. Like Navachab, the skarn mineralisation is situated at the contact to or within the shoshonites. Sheppard *et al.* (1995) emphasize the influence of the metasedimentary protolith on the mineralisation. They conclude, that the unusual mineralogy is the product of contact metamorphism and metasomatic alteration of metasediments and interbedded mafic volcanics.

Deposits like Navachab, Tillicum and Lucky Draw are distinct from Phanerozoic gold skarns associated with relatively shallow plutons. In older, Precambrian orogenic belts, metamorphism reaches relatively high temperatures. In addition, the pressure conditions indicate deeper levels more similar to W skarns rather than Au skarns. At Navachab, W occurs throughout the deposit as scheelite, confirming the similarities to W skarns. Meinert (1998) regards these deposits as hybrids between a regional metamorphic environment and phanerozoic plutonism. The role of mafic or ultramafic rocks in the vicinity of some of these deposits still needs further investigation.

Even in older orogenic gold belts, there are two main models for the association of gold mineralisation with an intrusion. The magmatic model (Burrows *et al.*, 1986) considers the intrusive body to be the source of the gold. The metamorphic model (Groves and Phillips, 1987) favours the leaching of gold from the intrusion due to the circulation of fluids. The occurrence of gold mineralisation in the vicinity of lamprophyres and the high contents of volatiles in lamprophyres led Rock and Groves (1988) to the conclusion, that lamprophyres represent the original transport media of gold-bearing fluids. Lamprophyres, however, seldom carry significant

amounts of gold and this is also the case for Navachab. Thus, the lamprophyre of Navachab is considered to represent a redox trap for the circulating gold-bearing fluids. The association of different types of skarns with different compositions of plutons (Meinert, 1995) suggests that most gold skarns are associated with calc-alkaline intrusions. At Navachab, the calc-alkaline basement rocks that crop out a few kilometers to the south in the Abbabis Inlier, may represent the original source of the gold and some of the Mn and Fe. Another possible source for the enrichment of Mn and Fe is the manganese iron formation layer in the Chuos Formation which occurs in the footwall of the deposit. Mueller (1988) describes similar associations of Au-bearing, skarn-hosted quartz veins with Fe-rich metabasalts, BIF's and komatiites in the Yilgarn craton.

Steven *et al.* (1994) suggested that the cooling ages of 490 Ma of biotite at the margin of hydrothermal veins represented the age of skarn mineralisation. However, this may represent the end of skarn formation. The lamprophyre sill, which predates skarn mineralization at Navachab, is strongly foliated and this foliation is related to the last deformation stage (D3 on a regional scale). A synkinematic genesis of the skarn is suggested by the growth of helicitic garnets, kinking of pyrrhotite and twinning of carbonate and bismuth. Recent dating of the early syntectonic Mon Repos diorite and leucogranites near Navachab by Moore and Jacob (1998) led them to the conclusion, that these 540 Ma intrusions represent the original source of the gold. They consider Navachab to be a sheeted vein mesothermal deposit, developed distal to its related intrusion. However, these intrusions do not host any significant gold mineralisation nor significant Fe-Cu sulphides. In contrast to the findings of Moore and Jacob (1998), there is a significant mineralogical zonation over the deposit, expressed by the increase of subcalcic garnets in central parts of the skarn (MC unit) that differs clearly from the composition of metamorphic garnets in the marble (M unit).

If the Damaran diorites and leucogranites are related to mineralization and skarn formation at Navachab and given the relatively large distance of fluid transport that this would require, it seems likely that the metal-bearing fluids of Navachab represent a mixture of fluid and metal sources, including those remobilised and derived from basement rocks. The key feature at Navachab is the presence of a lamprophyre that may have served as a redox trap for the circulating fluids. This commonly observed association of Palaeozoic-Proterozoic gold skarns with lamprophyres or related mafic-ultramafic rocks offers a new perspective for exploration strategies.

References

- Burrows, D.R., Wood, P.C. and Spooner, E.T. 1986. Carbon isotope evidence for an magmatic origin for Archaen Au-quartz vein ore deposits. *Nature*, **321**, 851-854.
- Erongo Mining and Exploration Company Ltd. 1989. *Navachab Gold Mine Guide*, Karibib-Namibia, 36 pp.
- Ettlinger, A.D. and Ray, G. 1989. Precious metal enriched skarns in British Columbia: an overview and geological study. *Province of British Columbia, Min. Res. Div. Pap.*, 1989-3.
- Gamble, R. 1982. An experimental study of sulfidation reactions involving andradite and hedenbergite. *Econ. Geol.*, **77**, 784-797.
- Groves, D.I. and Phillips, G.N. 1987. The genesis and tectonic control of archean gold deposits of the Western Australian Shield- a metamorphic replacement model. *Ore Geol. Rev.*, **2**, 287-322.
- Haack, U., Gohn, E. and Klein, J. 1980. Rb/Sr-ages of granitic rocks along the middle reaches of the Omaruru river and the timing of orogenic events in the Damara belt, Namibia. *Contr. Mineral. Petrol.*, **74**, 349-360.
- Hartnady, C.J., Joubert, P., Stowe, C. 1985. Proterozoic crustal evolution in southwestern Africa. *Episodes*, **8**, 236-244.
- Hoffer, E. 1983. Compositional variations of metapelites involved in low- to medium-grade isograd reactions in the Southern Damara Orogen, Namibia/S.W. Africa, 745-765. In: Martin, H. and Eder, F. (eds) *Intracontinental fold belts*. Springer, Berlin, 945 pp.
- Horstmann, U.E. 1987. Die metamorphe Entwicklung im Damara Orogen, SW-Afrika/Namibia, abgeleitet aus K/Ar-Datierungen an detritischen Hellglimmern aus Molassesedimenten der Nama-Group. *Göttinger Arb. Geol. Paläont.*, **31**, 92 pp.
- Hutchinson, M. and Scott, S.D. 1981. Sphalerite geobarometry in the Cu-Fe-Zn-S system. *Econ. Geol.*, **76**, 143-153.
- Jacob, R.E., Kroener, A. and Burger, A.J. 1978. Areal extent and first U-Pb-age of the predamara Abbabis Complex in the central Damara-belt of S.W. Africa (Namibia). *Geol. Rdsch.*, **67**, 706-718.
- Kretschmar, U. and Scott, S.D. 1976. Phase relations involving Arsenopyrite in the system Fe-As-S and their application. *Canad. Mineral.*, **14**, 364-386.
- Kröner, A. 1982. Rb/Sr geochronology and tectonic evolution of the Pan-African of Namibia. *Am. J. Sci.*, **282**, 1471-1507.
- Meinert, L.D. 1995. Compositional variations of igneous rocks associated with skarn deposits. In: Thompson, J. (ed.) *Magmas, Fluids and Ore deposits*. Mineral. Assoc. Can., Short Course, **23**, 401-418.
- Meinert, L.D. 1998. A Review of skarns that contain gold. In: Lentz, D.R. *Mineralized Intrusion-related Skarn systems*. Mineral. Assoc. Can., Short Course, **26**, 359-414.
- Miller, R.McG. 1983. Evolution of the Damara-Orogen of South West Africa/Namibia, 431-515. In: Miller, R.McG. (ed.) *Geodynamic evolution of the Damara*

- Orogen. Spec. Publ. geol. Soc. S. Afr., **11**, 515 pp.
- Milner, S., le Roex, A. and O'Corner, M. 1995. Age of Mesozoic igneous rocks in northwestern Namibia, and their relationship to continental breakup. *J. geol. Soc. London*, **152**, 97-104.
- Moore, J.M. and Jacob, R. E. 1998. The Navachab sheeted-vein/ skarn Au-deposit, Namibia. *Abstract GAC-MAC joint congress Quebec 1998*, A125-126.
- Mueller, A.G. 1988. Archaen gold-silver deposits with prominent calc-silicate alteration in the Southern Cross greenstone-belt, Western Australia: analogues of Phanerozoic skarn deposits. In: Ho, S.I. and Groves, D.I., *Advances in Understanding Precambrian Gold Deposits 2*. Geology Department, Univ. Western Australia, **12**, 141-163.
- Nakazawa, H. and N.Morimoto, N. 1971. Phase Relations and Superstructures of Pyrrhotite, Fe_{1-x}S. *Mat. Res. Bull.*, **6**, 345-358.
- Nörtemann, M.F.-J. 1997. *Geological mapping of the Goldkuppe area on the farms Otjimbojo and Otjakatjongo in the central Damara-Orogen, Namibia, & Genesis, Petrography and Mineral Chemistry of the Goldskarn deposit Navachab in the central Damara-Orogen, Namibia*. Unpubl. Diplom thesis, Univ. Göttingen, 265 pp.
- Pirajno, F. and Jacob, R.E. 1991. Gold mineralisation in the intracontinental branch of the Damara-Orogen, Namibia: a preliminary survey. *J. Afr. Earth Sci.*, **13**, 305-311.
- Porada, H. 1989. Pan-African rifting and orogenesis in southern to equatorial Africa and eastern Brazil. *Precamb. Res.*, **44**, 103-136.
- Puhan, D. 1983. Temperature and pressure of metamorphism in the central Damara-Orogen, 219-225. In: Miller, R.McG. (ed.) *Geodynamic evolution of the Damara Orogen*. Spec. Publ. geol. Soc. S. Afr., **11**, 515 pp.
- Rock, N.M.S. 1991. *Lamprophyres*. Blackie & Son, London, 285 pp.
- Rock, N.M.S. and Groves, D.I. 1988. Do Lamprophyres carry gold as well as diamonds? *Nature*, **332**, 253-255.
- Sheppard, S., Walshe, J.L. and Pooley, G.D. 1995. Non-carbonate, skarn-like Au-Bi-Te mineralization, Lucky Draw, New South Wales, Australia. *Econ. Geol.*, **90**, 1553-1569.
- Spry, A. 1973. *Metamorphic Textures*. Pergamon Press, Oxford, 350 pp.
- Steven, N.M. 1994. A review of gold occurrences in the northern and central zones of the Damara Orogen and the underlying mid-Proterozoic basement, central Namibia. *Communs geol. Surv. Namibia*, **9**, 63-77.
- Steven, N.M. and Moore, J.M. 1993. A Study of epigenetic mineralisation in the Central Zone of the Damara-Orogen, Namibia, with a special reference to gold, tungsten and rare earth elements. *Mem. geol. Surv. Namibia*, **16**, 166 pp.
- Steven, N.M., Kuyper, J.L. and Moore, J.M. 1994. Late Proterozoic and early Palaeozoic metasediment-hosted tungsten in central Namibia: recent advances in exploration and research. *Explor. Min. Geol.*, **3**, 337-348.